Robust Orthogonal Matching Pursuit Detector Applications to off-grid target issues in MIMO Radar

Laurent Savy, Mathieu Cattenoz, Sylvie Marcos

Robust Orthogonal Matching Pursuit Detector

Applications to off-grid target issues in MIMO Radar

Laurent Savy
Technical Directorate
Thales Airborne Systems
Elancourt, France
Laurent.savy@fr.thalesgroup.com

Mathieu Cattenoz, Sylvie Marcos
L2S
Gif-sur-Yvette, France
Mathieu.Cattenoz@ gmail.com
sylvie.marcos@l2s.centralesupelec.fr

***Abstract*—The paper proposes to solve the off-grid issue arising in sparse processing involving Orthogonal Matching Pursuit (OMP) algorithm. It starts by establishing the Generalized Likelihood Ratio Test using a stochastic model to represent target location uncertainty within one resolution cell. In a second step, a linear approximate of the detector is built, requiring only a grid oversampling of 2 relative to the resolution cell size. Moreover, it involves only the formation of standard delta channels in each dimension, leading to low computational burden without loss of efficiency. The approach is here demonstrated on MIMO radar detection.**

Keywords: Orthogonal Matching Pursuit; off-grid target; MIMO radar;

I. INTRODUCTION

In conventional radar processing, since the target parameters (for instance range, Doppler or angle) are unknown, different matched filter operations (range matched filter, Doppler processing, array beamforming) are applied for different parameter hypotheses in order to retrieve the target. This matched filter is mainly derived in the single target hypothesis and is however used in multi-targets environment with loss of processing. This usually consists in adding standard weighting windows onto the filter in order to lower the side lobes level of the mismatched filtering. In addition, the different single-source assumptions define a grid in the parameter space and the targets are never exactly on the resolution grid, causing a loss of processing due to a shift between the nearest grid point and the real target steering vector. However, for the specific kind of signals encountered in radar, the average losses over all target position within a resolution cell with conventional weighting functions are generally contained below 3dB. Theses losses are traditionally accepted to save computational load and remain in the most manageable case of the multiple single-source assumptions for detection with noise independence assumptions, which also allow the theoretical calculation of the threshold for the control of the false alarm probability.

However, in some situations, it appears that the mismatched filter in the multi-targets environment leads to poor performance and is not practical~~,~~ due to the inability to find efficient apodization techniques. This is the case when the signal model deviates significantly form the linear phase complex exponential, found in particular in coherent MIMO radars where the range and angle dimensions are coupled due to the non-perfect orthogonality of the waveforms [1].

In this situation, the main idea is to find a feasible approximate implementation of the global matched filter in the context of sparse targets hypothesis. In presence of spread non-point targets, a relevant solution is the Orthogonal Matching Pursuit (OMP) algorithm, see for instance [2]. Because the projector onto the space orthogonal to one target steering vector is very sharp, the standard OMP solution requires ~~to~~ severe oversampling to mitigate the off-grid target issue. Anyway, in case of closely spaced targets (typically less than one resolution cell), estimation of target signal in the detection step becomes so biased that the rejection step can only perform poorly and spurious detections may occur. In [2,3], the authors proposed to mitigate the off-grid issue by using in the OMP rejection step the space spanned by the entire resolution cell. Unfortunately, the proposed methods are mainly dedicated to the case of steering vectors being complex exponential with linear phase evolution, otherwise computational load will become prohibitive.

In [4] we proposed to mitigate the off-grid issue by using in the OMP rejection step the space spanned by adjacent steering vectors of a half cell. The basic idea is to enlarge the rejection region in the OMP rejection step. The method has been proven to work well on real data, to be computationally very efficient, and was justified using the development in Taylor series at second order of the steering vector in [5].

In this paper we go much deeper in the previous justification, showing the link with the Generalized Likelihood Ratio Test (GLRT) for target arbitrary localized within one resolution cell (or extended target) and deriving the discrete formulation of the detector in the Low Energy Coherence (LEC) case, already established for continuous signal in [6]. This is detailed in section II.

In section III, using the Taylor series development of the steering vectors in one resolution cell, we show that the space spanned by one resolution cell can be well defined by few steering vectors. It is furthermore shown that the computation of these steering vectors only requires an oversampling by two

of the conventional one-cell grid, for the majority of practical radar waveforms and/or radar antenna configurations.

Section IV, illustrates in more details the application of the proposed method to the coherent MIMO radar detection processing, involving OMP algorithm.

II. LOW COHERENCE ENERGY CASE DETECTOR FOR OFF-GRID TARGET – IMPACT ON OMP REJECTION STEP

A. Standard matched filter and OMP

As a clarification, we recall that the standard canonical hypothesis testing (i.e. on whitened data) for point target leading to the matched filter is the following situation:

$$\begin{aligned} H_0 &: \quad \mathbf{x} = \mathbf{n} \quad (\textit{noise only}) \qquad \mathbf{n} \sim \mathcal{CN}(0, \mathbf{Id}) \\ H_1 &: \quad \mathbf{x} = \alpha \mathbf{s}(\boldsymbol{\theta}_0) + \mathbf{n} \quad (\textit{signal} + \textit{noise}) \end{aligned} \tag{1}$$

α is the unknown target complex amplitude and $\mathbf{s}(\boldsymbol{\theta}_0)$ is the steering vector, depending on a vector of parameters. $\boldsymbol{\theta}_0 = [\theta_{01}\ \theta_{02} \cdots \theta_{0P}]^T$. $\boldsymbol{\theta}_0$ =(range, and/or Doppler frequency, and/or angles) in radar detection problems.

The GLRT for detection is then the matched filter:

$$Y(\boldsymbol{\theta}_0) = \frac{\left|\mathbf{s}^H(\boldsymbol{\theta}_0)\mathbf{x}\right|^2}{\mathbf{s}^H(\boldsymbol{\theta}_0)\mathbf{s}(\boldsymbol{\theta}_0)} \underset{H_0}{\overset{H_1}{\gtrless}} \eta \quad (\eta\ \textit{threshold}) \tag{2}$$

$\boldsymbol{\theta}_0$ is usually sampled on a grid with mesh corresponding to a resolution cell. The OMP algorithm built on the previous model is then an iterative implementation of the multi-target matched filter that consists in detecting and rejecting each contribution of the strongest targets successively. It starts with $\mathbf{x}^1 = \mathbf{x}$ and the k[th] iteration of the procedure can be summarized by the two following steps:

$$\begin{aligned} &\text{Detection step}: \text{find } \boldsymbol{\theta}_0^k = \underset{\boldsymbol{\theta}_0}{\text{Argmax}} \frac{\left|\mathbf{s}^H(\boldsymbol{\theta}_0)\mathbf{x}^k\right|^2}{\mathbf{s}^H(\boldsymbol{\theta}_0)\mathbf{s}(\boldsymbol{\theta}_0)} \\ &\text{Rejection step}: \quad \mathbf{A}_k = \left[\mathbf{A}_{k-1}, \mathbf{s}(\boldsymbol{\theta}_0^k)\right], \quad \mathbf{A}_0 = [\,] \\ &\qquad\qquad \mathbf{x}^{k+1} = (\mathbf{I} - \mathbf{A}_k(\mathbf{A}_k^H\mathbf{A}_k)^{-1}\mathbf{A}_k^H)\mathbf{x} \end{aligned} \tag{3}$$

B. Low Coherency Energy detector and impact on OMP

In order to deal with the off-grid issue, we first change the target deterministic model in hypothesis H_1 to a stochastic one as follow:

$$H_1: \quad \mathbf{x} = \mathbf{t} + \mathbf{n} \quad \mathbf{t} \sim \mathcal{CN}(0, \sigma^2\mathbf{S}(\boldsymbol{\theta}_0)),\ \mathbf{n} \sim \mathcal{CN}(0, \mathbf{Id})$$

$$\mathbf{S}(\boldsymbol{\theta}_0) = \int_{\theta_{01}-\frac{\Delta\theta_1}{2}}^{\theta_{01}+\frac{\Delta\theta_1}{2}} \cdots \int_{\theta_{0P}-\frac{\Delta\theta_P}{2}}^{\theta_{0P}+\frac{\Delta\theta_P}{2}} \mathbf{s}(\boldsymbol{\theta})\mathbf{s}^H(\boldsymbol{\theta}) d\boldsymbol{\theta} \tag{4}$$

$\mathbf{S}(\boldsymbol{\theta}_0)$ is the normalized power known covariance matrix of the target, according to the possibility for the target to fall anywhere in one resolution cell defined by $\Delta\boldsymbol{\theta} = [\Delta\theta_1\ \Delta\theta_2 \cdots \Delta\theta_P]^T$ around $\boldsymbol{\theta}_0 = [\theta_{01}\ \theta_{02} \cdots \theta_{0P}]^T$. σ^2 is the unknown target power. It is worth noting that this model can also be used for extended target detection or for modeling steering vectors uncertainties (by adding extra parameters in steering vector model in the last case).

The likelihood ratio test with this stochastic model can be written now after some operations:

$$\mathbf{x}^H(\mathbf{Id} - (\mathbf{Id} + \sigma^2\mathbf{S}(\boldsymbol{\theta}_0))^{-1})\mathbf{x} \underset{H_0}{\overset{H_1}{\gtrless}} \eta\ Log\left|\mathbf{Id} + \sigma^2\mathbf{S}(\boldsymbol{\theta}_0)\right| \tag{5}$$

Denoting the singular value decomposition of $S(\boldsymbol{\theta}_0)$ by:

$$\begin{aligned} &\mathbf{S}(\boldsymbol{\theta}_0) = \sum_n \lambda_n \mathbf{v}_n \mathbf{v}_n^H \quad n = 1:N \quad NxN: \text{size of } \mathbf{S}(\boldsymbol{\theta}_0) \\ &(\mathbf{Id} + \sigma^2\mathbf{S}(\boldsymbol{\theta}_0))^{-1} = \mathbf{Id} - \sum_n \frac{\sigma^2\lambda_n}{\sigma^2\lambda_n + 1}\mathbf{v}_n\mathbf{v}_n^H \\ &Log\left|\mathbf{Id} + \sigma^2\mathbf{S}(\boldsymbol{\theta}_0)\right| = \sum_n Log(\sigma^2\lambda_n + 1) \end{aligned} \tag{6}$$

After some more operations, the likelihood ratio test (5) can be finally written as :

$$\sum_n \frac{\sigma^2\lambda_n}{\sigma^2\lambda_n + 1}\left|\mathbf{v}_n^H\mathbf{x}\right|^2 \underset{H_0}{\overset{H_1}{\gtrless}} \eta \sum_n Log(\sigma^2\lambda_n + 1) \tag{7}$$

It is worth noting that (7) is a weighted and generalized version of the subspace-based matched detector [6], where projections on the eigenvectors of $\mathbf{S}(\boldsymbol{\theta}_0)$ accounts for signal to noise ratio in each eigenvector related subspace. Only in the case of a strong target and a limited number of non-zero eigenvalues of $\mathbf{S}(\boldsymbol{\theta}_0)$ we recover the matched subspace detector of [6]. One can also note that we recover the matched filter of (2) in case $\mathbf{S}(\boldsymbol{\theta}_0)$ is of rank 1 and in that case (4) is simply written as $\mathbf{S}(\boldsymbol{\theta}_0) = \mathbf{s}(\boldsymbol{\theta}_0)\mathbf{s}^H(\boldsymbol{\theta}_0) = \mathbf{v}_0\mathbf{v}_0^H$.

More interesting is the case of weak target (much below the noise), where we can get rid of the target power σ^2 in the test (7). Indeed, for weak target the test leads to:

$$\frac{\sum_n \lambda_n\left|\mathbf{v}_n^H\mathbf{x}\right|^2}{\sum_n \lambda_n} = \frac{\mathbf{x}^H\mathbf{S}(\boldsymbol{\theta}_0)\mathbf{x}}{Tr\{\mathbf{S}(\boldsymbol{\theta}_0)\}} \underset{H_0}{\overset{H_1}{\gtrless}} \eta \tag{8}$$

$$\text{because } \frac{\sigma^2\lambda_n}{\sigma^2\lambda_n + 1} \approx \sigma^2\lambda_n \textit{ and } Log(\sigma^2\lambda_n + 1) \approx \sigma^2\lambda_n$$

Equation (8) shows that for weak target the detector simply turns to the weighted average of the projections onto the eigenvectors of $\mathbf{S}(\boldsymbol{\theta}_0)$ by the eigenvalues. In our situation of

interest, where $\mathbf{S}(\boldsymbol{\theta}_0)$ describes the signal in one resolution cell, the λ_n's in (6) decrease very rapidly.

Equation (8) then can be reduced with little loss to the first term in the sum for detection purpose. However, for enough rejection of signal falling in one resolution, as required for OMP algorithm rejection step, a few more eigenvectors are needed. The OMP procedure with the stochastic target model then becomes:

$$\begin{aligned}&\text{Detection step: find } \boldsymbol{\theta}_0^k = \underset{\boldsymbol{\theta}_0}{\text{Argmax}} \frac{\left|\mathbf{s}^H(\boldsymbol{\theta}_0)\mathbf{x}^k\right|^2}{\mathbf{s}^H(\boldsymbol{\theta}_0)\mathbf{s}(\boldsymbol{\theta}_0)}\\ &\text{Rejection step: } \quad \mathbf{A}_k = \left[\mathbf{A}_{k-1}, \mathbf{V}_s^k\right]\\ &\qquad\qquad \mathbf{x}^{k+1} = (\mathbf{I} - \mathbf{A}_k(\mathbf{A}_k^H\mathbf{A}_k)^{-1}\mathbf{A}_k^H)\mathbf{x}\end{aligned} \tag{9}$$

$\mathbf{V}_s^k = \left[\mathbf{v}_0^k, \cdots, \mathbf{v}_{M-1}^k\right]$: matrix formed by the eigenvectors corresponding to the M dominant eigenvalues of $\mathbf{S}(\boldsymbol{\theta}_0^k)$ that are sufficient to get enough cancelation of all the signals within one resolution cell.

C. *Illustration on mono dimensional complex exponential signal with linear phase*

The previous results are illustrated for the particular but relevant case of a mono dimensional complex exponential with linear phase for signal $\mathbf{s}(\boldsymbol{\theta})$, which can represent in radar Doppler analysis, range compression, or antenna beamforming on a uniform linear array. In that case:

$$\mathbf{s}(\theta) = \left[\, e^{-i2\pi\frac{\theta}{N}\frac{(N-1)}{2}} \cdots e^{i2\pi\frac{\theta}{N}(n-\frac{(N-1)}{2})} \cdots e^{i2\pi\frac{\theta}{N}\frac{(N-1)}{2}} \right]^T \tag{10}$$

n can represent either the pulse index in Doppler analysis, the frequency bin index in pulse compression, or the antenna element index in a linear uniformly space array. θ represents then respectively the Doppler bin index, the range bin index, or the angle bin index. The resolution cell extent is defined by $\Delta\theta = 1$ and due to the nature of $\mathbf{s}(\theta)$:

$\mathbf{S}(\theta_0) = \left[\mathbf{s}(\theta_0)\mathbf{s}^H(\theta_0)\right] \odot \mathbf{S}(0)$, with $\odot$: Hadamard product.

In that particular case, the eigenvalues of $\mathbf{S}(\boldsymbol{\theta}_0)$ are the same than the ones of $\mathbf{S}(0)$, and the n^{th} eigenvector $\mathbf{v}_n(\theta_0)$ of $\mathbf{S}(\theta_0)$ is equal to $\mathbf{s}(\theta_0) \odot \mathbf{v}_n(0)$, with $\mathbf{v}_n(0)$ the n$^{\text{th}}$ eigenvector of $\mathbf{S}(0)$. The eigenvalues of $\mathbf{S}(0)$ are plotted for illustration on Fig. 1. It is clear that most of the energy is captured by the first eigenvector with 80% (-1dB) of the total energy (see zoom on the first eigenvalues).

In next section, using 1$^{\text{st}}$ order and 2$^{\text{nd}}$ order expansion of the steering vector in one resolution cell, we show that the space spanned by one resolution cell can be well defined by only two or three steering vectors for each parameter. It leads to a very computationally efficient implementation of the projection of the signal in the space orthogonal to one resolution cell, needing only an oversampling by 2 of the standard one-cell stepped grid.

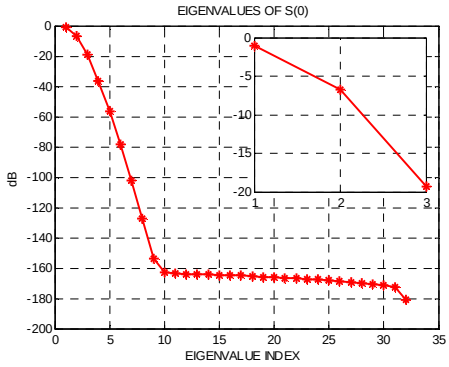

Fig. 1 Eigenvalues of S(0) for complex exponential signal with N=32

III. APPROXIMATE SPACE SPANNED BY ONE CELL

A. *Taylor series expansion approximate*

We start here by 1$^{\text{st}}$ and 2$^{\text{nd}}$ order linear approximation of the steering vector, quite valid in one resolution cell, around the value $\boldsymbol{\theta}_0$ (the center of the resolution cell):

$$\begin{aligned}\mathbf{s}(\boldsymbol{\theta}) &= \mathbf{s}(\boldsymbol{\theta}_0) + \sum_p (\theta_p - \theta_{0p}) \left.\frac{\partial \mathbf{s}(\boldsymbol{\theta})}{\partial \theta_p}\right|_{\boldsymbol{\theta}=\boldsymbol{\theta}_0} \quad 1^{st} \text{ order}\\ &+ \frac{1}{2}\sum_p\sum_\ell (\theta_p - \theta_{0p})(\theta_\ell - \theta_{0\ell}) \left.\frac{\partial^2 \mathbf{s}(\boldsymbol{\theta})}{\partial \theta_p \partial \theta_\ell}\right|_{\boldsymbol{\theta}=\boldsymbol{\theta}_0} \quad 2^{nd} \text{ order}\end{aligned} \tag{11}$$

Clearly the spaced defined by the vectors $\mathbf{s}(\boldsymbol{\theta}_0), \left.\frac{\partial \mathbf{s}(\boldsymbol{\theta})}{\partial \theta_p}\right|_{\boldsymbol{\theta}=\boldsymbol{\theta}_0}, \left.\frac{\partial^2 \mathbf{s}(\boldsymbol{\theta})}{\partial \theta_p \partial \theta_\ell}\right|_{\boldsymbol{\theta}=\boldsymbol{\theta}_0}$ is the best approximation at order 2 of the space spanned by one resolution cell. In the same way, the corresponding approximation of $\mathbf{S}(\boldsymbol{\theta}_0)$ is obtained by using the expressions of $\mathbf{s}(\boldsymbol{\theta})$ in (11) to compute (4). Note however that these vectors do not correspond necessarily to the eigenvectors of the approximation of $\mathbf{S}(\boldsymbol{\theta}_0)$ since there are not orthogonal in the general case. Actually only $\mathbf{s}(\boldsymbol{\theta}_0)$ *and* $\left.\frac{\partial \mathbf{s}(\boldsymbol{\theta})}{\partial \theta_p}\right|_{\boldsymbol{\theta}=\boldsymbol{\theta}_0}$ are orthogonal in the general case due to the maximum of the ambiguity function in $\boldsymbol{\theta} = \boldsymbol{\theta}_0$, and only in case of non-coupled parameters $\left.\frac{\partial \mathbf{s}(\boldsymbol{\theta})}{\partial \theta_p}\right|_{\boldsymbol{\theta}=\boldsymbol{\theta}_0}$ *and* $\left.\frac{\partial \mathbf{s}(\boldsymbol{\theta})}{\partial \theta_\ell}\right|_{\boldsymbol{\theta}=\boldsymbol{\theta}_0}$, $p \neq \ell$ are also orthogonal (usual case case for range/angle/Doppler dimensions in radar, except in the MIMO case, or except with Doppler effect on the pulse). This means that for regular radar cases, the first order expansion of the steering vector corresponds also to the eigenvector decomposition of the first order approximate of $\mathbf{S}(\boldsymbol{\theta}_0)$.

B. *Efficient computation of the projector on the space othogonal to one resolution cell via difference channels*

From the previous section, it is clear that to compute an approximate projection on the space orthogonal to one resolution cell, needed for the rejection step in OMP, we have for each hypothesis $\boldsymbol{\theta}_0$ to compute P+1 "channels" at 1st order and P+1 + P(P+1)/2 channels at 2nd order defined by:

$$\begin{aligned}
&\mathbf{s}_0^H\mathbf{x}: \text{"}sum\text{"}\ channel \qquad \mathbf{s}_0 = \mathbf{s}(\boldsymbol{\theta}_0)\\
&\partial\mathbf{s}_p^H\mathbf{x}: 1^{st}\ order\text{"}delta\text{"}\ channels \quad \partial\mathbf{s}_p = \left.\frac{\partial\mathbf{s}(\boldsymbol{\theta})}{\partial\theta_p}\right|_{\boldsymbol{\theta}=\boldsymbol{\theta}_0}\\
&\partial^2\mathbf{s}_p^H\mathbf{x}: 2^{nd}\ order\ \text{"}delta\text{"}\ channels \quad \partial^2\mathbf{s}_p^H = \left.\frac{\partial^2\mathbf{s}(\boldsymbol{\theta})}{\partial\theta_p\partial\theta_\ell}\right|_{\boldsymbol{\theta}=\boldsymbol{\theta}_0}
\end{aligned} \tag{12}$$

and to use, for rejection step in OMP, the matrix:

$$\begin{aligned}
&\mathbf{V}_s = \left[\mathbf{s}_0\ \partial\mathbf{s}_1 \cdots \partial\mathbf{s}_P\ \right] \qquad at\ \ 1^{st}\ \text{order}\\
&\mathbf{V}_s = \left[\mathbf{s}_0\ \partial\mathbf{s}_1 \cdots \partial\mathbf{s}_P\ \ \partial^2\mathbf{s}_1 \cdots \partial^2\mathbf{s}_P\right] \quad at\ \ 2^{nd}\ \text{order}
\end{aligned} \tag{13}$$

In order to compute very efficiently the delta channels $\mathbf{V}_S^H\mathbf{x}$ (and hence the rejection step), we approximate them by finite differences derived from a twice oversampled grid to get half resolution cells.

For a mono-dimensional signal, as the one in (10), this approximation is written classically as:

$$\begin{aligned}
\left.\frac{\partial\mathbf{s}(\theta)}{\partial\theta}\right|_{\theta=\theta_0} &\approx \frac{\mathbf{s}(\theta_0+\frac{\Delta\theta}{2})-\mathbf{s}(\theta_0-\frac{\Delta\theta}{2})}{\Delta\theta}\\
\left.\frac{\partial\mathbf{s}^2(\theta)}{\partial\theta^2}\right|_{\theta=\theta_0} &\approx \frac{\mathbf{s}(\theta_0+\frac{\Delta\theta}{2})-2\mathbf{s}(\theta_0)+\mathbf{s}(\theta_0-\frac{\Delta\theta}{2})}{\Delta\theta^2/4}
\end{aligned} \tag{14}$$

To compare the efficiency of the projections defined by (13) and its approximates defined by (14), we took the same signal example as in Fig. 1, and computed the projector response $\mathbf{s}^H(\theta)(\mathbf{Id}-\mathbf{V}_s(\mathbf{V}_s^H\mathbf{V}_s)^{-1}\mathbf{V}_s^H)\mathbf{s}(\theta)$, and added also the standard OMP projector using only $\mathbf{V}_s=\mathbf{s}_0$. The results are plotted on Fig. 2. Clearly the delta channel projectors avoid the sharpness of the standard projector, while preserving a deep notch. It can be seen also that the approximate delta channels of (12) are closed to the exact delta channels of (11), which validates the proposed approach.

It is worth noting that at 2nd order we get the same projector using the delta channels defined by (14) in $\mathbf{V}_s$ or using directly

$$\mathbf{V}_s = \left[\mathbf{s}_0\ \ \mathbf{s}(\theta_0+\frac{\Delta\theta}{2})\ \ \mathbf{s}(\theta_0-\frac{\Delta\theta}{2})\ \right] \tag{15}$$

Indeed the delta channels are a linear combination of the three vectors involved in (15). This latest formulation is the half-cell projector already identified in an heuristic way in [4].

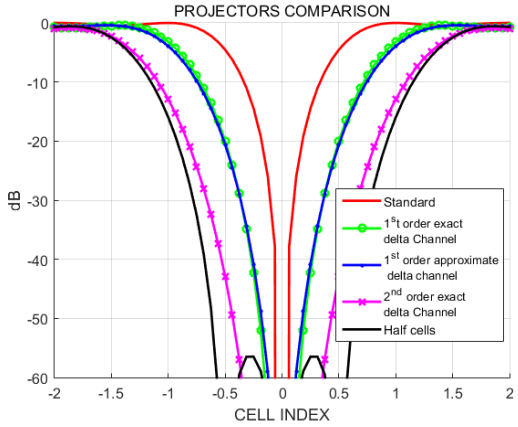

Fig. 2 Projectors comparison

IV. APPLICATION TO MIMO RADAR PROCESSING

In this section we will first briefly review the coherent MIMO radar with intrapulse coding and the associated sidelobes issues of the ambiguity function (to go further, detailed discussions can be found for instance in [1]). In a second step, we will then give some applications of the technique described in III on simulated and real MIMO data.

A. *Brief review of coherent MIMO radar processing and ambiguity function*

For the sake of simplicity, let us consider a transmitting linear array composed of M colocated isotropic antennas. In a conventional phased array, all antennas transmit the same waveform, and only the phases of the waveforms are different to form the beam in a given direction. In coherent colocated intrapulse coding MIMO radar, each of the M antennas transmits a different pulsed waveform $s_m(t)$, with repetition interval T_R so that the signal transmitted by the array in target located at direction θ_c is given by:

$$s_E(t,\theta_c) = \sum_\ell \sum_{m=1}^{M} e^{i\mathbf{k}^T(\theta_c)\mathbf{x}_{E,m}} s_m(t-\ell T_R) \tag{16}$$

where $\mathbf{x}_{E,m}$ is a vector representing the position of the m^{th} antenna, and $\mathbf{k}(\theta_c)$ is the wave vector.

Let us now assume without lack of generality that the receive array is composed of one isotropic antenna. Indeed it is shown in [8] that the angular reception processing can be completely decoupled. Then the received signal from a target of unknown amplitude α, with delay $\tau_c = 2r/c$ (r is target range) and Doppler frequency υ_c is provided by:

$$x(t) = \alpha s(t,\tau_c,\theta_c,\upsilon_c) + b(t) \quad \text{with } b(t) \text{ the noise}$$

$$s(t,\tau_c,\theta_c,\upsilon_c) = \sum_\ell \sum_{m=1}^{M} e^{i\mathbf{k}^T(\theta_c)\mathbf{x}_{E,m}} s_m(t-\ell T_R-\tau_c) e^{i2\pi\upsilon_c t}$$

Then, the response of the matched filter at the output of the receiver is:

$$y(\tau,\theta,\upsilon)=\sum_{\ell'}\sum_{m'=1}^{M} e^{-i\mathbf{k}^T(\theta)\mathbf{x}_{E,m'}}\int x(t)s^*_{m'}(t-\ell T_R-\tau)e^{-i2\pi\upsilon t}$$

Moreover it is also shown in [8] that in case of no Doppler effect on the pulse, the Doppler processing can be completely decoupled from the range-angle processing, and that what matters in coherent MIMO processing is the range-angle matched filter for one elementary pulse given by:

$$y(\tau,\theta)=\sum_{m'=1}^{M} e^{-i\mathbf{k}^T(\theta)\mathbf{x}_{E,m'}}\int x(t)s^*_{m'}(t-\tau)dt$$

We can derive from the above equations established in continuous time the formulation for discrete signals with sampling period *Te*. The signal model we need for matched filtering and OMP processing can be written as:

$$\mathbf{s}(\boldsymbol{\theta})=\mathbf{s}(\tau,\theta)=\mathbf{S}_w(\tau)\mathbf{s}_S(\theta)$$

$$(\mathbf{s}_S(\theta))_m=e^{i\mathbf{k}^T(\theta)\mathbf{x}_{E,m}},\quad \mathbf{s}_S: Mx1 \text{ spatial steering vector}$$

$$(\mathbf{S}_w(\tau))_{n,m}=s_m(nT_e-\tau),\quad \mathbf{S}_w(\tau): NxM \text{ waveform matrix}$$

The matched filter expressed in digital formalism is:

$$y(\tau,\theta)=\mathbf{s}^H(\boldsymbol{\theta})\mathbf{x}=\mathbf{s}(\tau,\theta)=\mathbf{s}_S^H(\theta)\mathbf{S}_w^H(\tau)\mathbf{x}$$

And the corresponding ambiguity function is:

$$\mathrm{X}(\tau-\tau_c,\theta,\theta_c)=\mathbf{s}_S^H(\theta)\left(\mathbf{S}_w^H(\tau)\mathbf{S}_w(\tau_c)\right)\mathbf{s}_S(\theta_c)$$

The matrix $\left(\mathbf{S}_w^H(\tau)\mathbf{S}_w(\tau_c)\right)=\tilde{\mathbf{S}}(\tau-\tau_c)$ of size *MxM* is the time cross-correlation matrix of the waveforms, and is not a diagonal matrix with practical waveforms, inducing range-angle coupling in coherent MIMO radar. Note also that the ambiguity function is a 3D function, depending on tested angle θ and actual target angle θ_c. Only hypothetic unrealizable orthogonal waveforms, with same autocorrelation function $C_{ss}(\tau)$ gives $\mathbf{S}_w^H(\tau)\mathbf{S}_w(\tau_c)=\mathrm{diag}(C_{ss}(\tau-\tau_c))$ and then a decoupled range-angle ambiguity function (see [1] for details):

$$\mathrm{X}^{decoupled}(\tau-\tau_c,\theta-\theta_c)=\mathbf{s}_S^H(\theta)\mathbf{s}_S(\theta_c)\cdot C_{ss}(\tau-\tau_c)$$

However, some waveform families may approach this condition. Among these families, an interesting case is provided by the Code Division Multiple Access (CDMA) phase codes used in digital communications [1]. For instance Gold codes which are optimized for having good periodic auto and cross correlation also provide good aperiodic correlations. Fig. 3 presents the range/angle 2D cut of the ambiguity function for τ_c=0 and θ_c =0 with Gold codes with N=127 chips, M=12 transmitters, pulse duration *Tp*=100µs, and bandwidth *B*=2 MHz. This set of parameters will be used further throughout the rest of the paper.

We observe a thumbtack type MIMO ambiguity function instead of a 2D sinc function in the ideal decoupled case. There is no noticeable coupling effect (so we get the full resolution in range and angle) but the energy is spread over the entire parameter space with high sidelobe level. This spreading comes from the summation of the non-zero cross correlations of the codes. This spreading can moreover not be mitigated with the use of conventional techniques of apodization windows.

There is therefore a strong need to decrease this level in multi-target environment to avoid the masking of weak targets by the sidelobes of strong targets. In the next paragraph, we present benefits provided by the robust OMP technique detailed in section III for that goal.

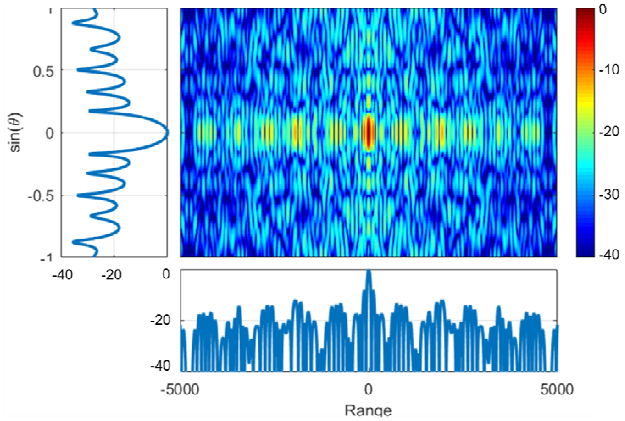

Fig. 3 – Range/angle cut of the MIMO ambiguity function for CDMA Gold codes of length N=127, N=12 transmitters, Tp=100µs, B=2 MHz

B. Extension of Robust OMP to MIMO radar

First we have to extend the approach of finite differences approximation defined in (14) for 1D on a 2D half-cell mesh grid. It was found, due to the finite differences approximation, that sufficient nulling of the space spanned by one cell requires not only to compute the regular 1st and 2nd order differences on each axes (4 parameters), but also the 1st and 2nd order differences obtained after a rotation of 45° of the parameter plane (4 additional parameters). This is equivalent to take for $\mathbf{V}_S$ in (13) the cell under test and its eight neighbors on a half-cell mesh grid. This is the direct extension of (14) in 1D (2 neighbors) to 2D (eight neighbors). The rationale is described in detail in [5]. The extended projector response, $\mathbf{s}^H(\tau,\theta)(\mathbf{Id}-\mathbf{V}_S(\mathbf{V}_S^H\mathbf{V}_S)^{-1}\mathbf{V}_S^H)\mathbf{s}(\tau,\theta)$, and the standard OMP projector using $\mathbf{V}_S=\mathbf{s}(\tau_0,\theta_0)$ are plotted on Fig. 4. Clearly the notch covers one resolution cell with a sufficient depth of almost 60dB.

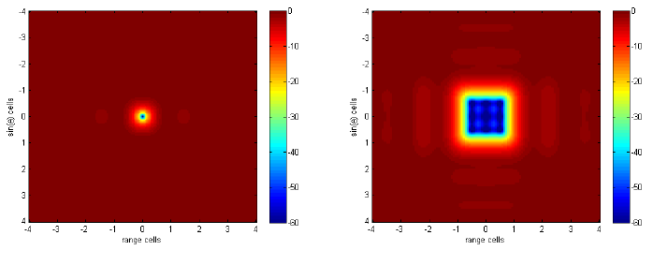

Fig. 4 – 2D standard (left) and extended (right) projector responses

C. *Results on simulated data of Robust OMP for MIMO radar detection*

In order to test the effectiveness of the robust OMP method, i.e. how the filter manages difficult situations, we use a particular scenario with two strong targets (same output SNR of 40 dB) with a decreasing distance *d* from 1.5 to 0.25 with steps of 0.25 range cell distances, and with a third weak target hidden in the sidelobes of the matched filter (output SNR of 15dB), located on a grid node in (-300m ; 0). The left-hand strong target is fixed on a grid node, while the right-hand strong target has a changing position, localized on a node only when its distance to the left target is a multiple of 0.5 cell width. We compute for each scenario the matched filter output, the standard OMP output and the proposed robust OMP output. These results are displayed on Fig. 5, Fig. 6, and Fig. 7 respectively. The proposed robust OMP avoids the spurious generation with standard OMP in case of closed or off-grid targets, and behaves as the matched filter for closed target within one resolution cell, giving only one detection. It also recovers well the weak target hidden in the sidelobes of the matched filter. In [5] the approach is also demonstrated on real data.

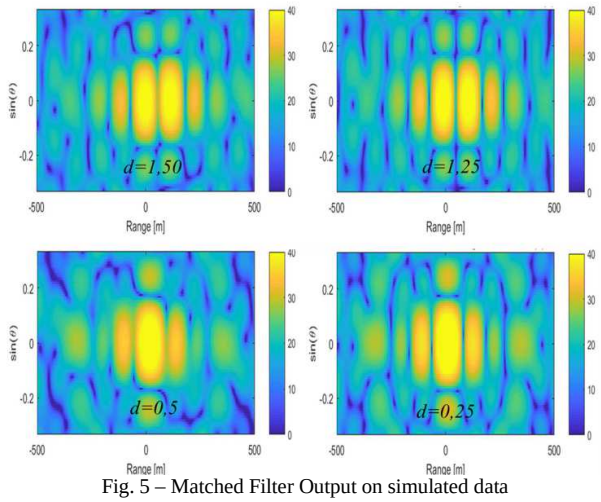

Fig. 5 – Matched Filter Output on simulated data

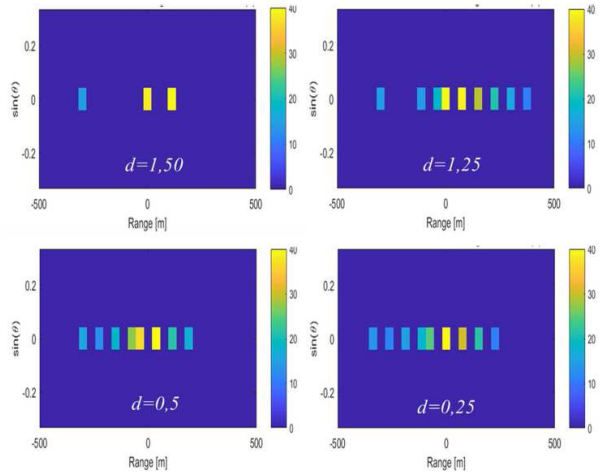

Fig. 6 – Standard OMP Output on simulated data

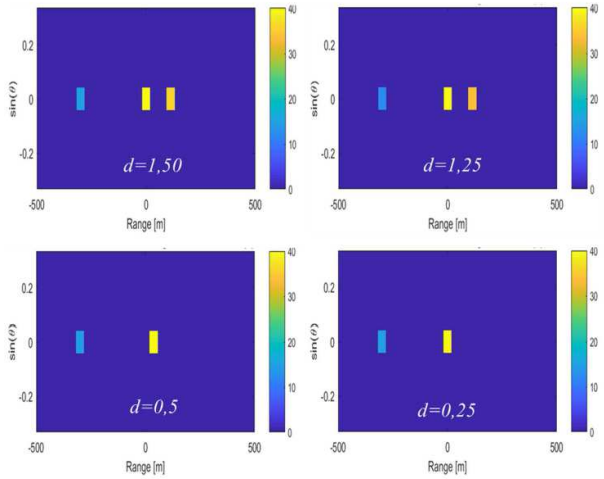

Fig. 7 Robust OMP Output on simulated data

V. CONCLUSION

In this paper we derived a robust version of OMP algorithm against off-grid/closed targets issues, justified with a stochastic model on targets relative to their location within one resolution cell in the parameter test grid. We have proposed a low computational load implementation involving only a half-cell mesh oversampled grid. The approach was demonstrated on simulated MIMO radar data. In [5] results on real data are given and it is also shown that the proposed method can be extended to model mismatch arising from hardware imperfect knowledge/calibration by incorporating small variants of the steering vector in the computation of (4).

REFERENCES

[1] Olivier Rabaste; Laurent Savy; Mathieu Cattenoz; Jean-Paul Guyvarch ; Signal waveforms and range/angle coupling in coherent colocated MIMO radar, 2013 International Conference on Radar

[2] J. Bosse, O. Rabaste, and D. Poullin, "Matching pursuit via continuous resolution cell rejection in presence of unresolved radar targets", 2015 23rd European Signal Processing Conference (EUSIPCO).

[3] O. Rabaste, J. Bosse and J.P. Ovarlez, "Off-Grid Target Detection With Normalized Matched Subspace Filter", 2016 24th European Signal Processingà Conference (EUSIPCO).

[4] Mathieu Cattenoz; Laurent Savy; Sylvie Marcos, Adaptive processing methods for MIMO radar experimental signals, 2014 IEEE International Radar Conference

[5] M. Cattenoz, L. Savy, and S. Marcos, Extended orthogonal matching pursuit for robust and fast target localisation in multiple-input multiple-output radar, IET Radar, Sonar & Navigation, Volume 11, issue 11, November 2017, p. 1709-1717

[6] Harry L. Van Trees, “Detection, Estimation, and Modulation Theory, Part III: Radar-Sonar Signal Processing and Gaussian Signals in Noise”, p 131, 2001 Wiley & Sons, Inc.

[7] L.L. Scharf and L.T. McWhorter, “Adaptive matched subspace detectors and adaptive coherence estimators”, Signals, Systems and Computers, 1996. Conference Record of the Thirtieth Asilomar Conference on.

[8] C. Chen and P. Vaidyanathan, “MIMO Radar Ambiguity Properties and Optimization Using Frequency-Hopping Waveforms,” IEEE Trans. On Signal Processing, vol. 56, no. 12, pp. 5926–59 368, 2008.